Journal of Zhejiang University-SCIENCE C (Computers & Electronics)
ISSN 1869-1951 (Print); ISSN 1869-196X (Online)
www.zju.edu.cn/jzus; www.springerlink.com
E-mail: jzus@zju.edu.cn

New separation algorithm for touching grain kernels based on contour segments and ellipse fitting*

Lei YAN[1,2], Cheol-Woo PARK[1], Sang-Ryong LEE[1], Choon-Young LEE[†‡1]

([1]*School of Mechanical Engineering, Kyungpook National University, Daegu 702-701, Korea*)

([2]*School of Technology, Beijing Forestry University, Beijing 100083, China*)

[†]E-mail: cylee@knu.ac.kr

Received Dec. 29, 2009; Revision accepted Apr. 29, 2010; Crosschecked Dec. 6, 2010

Abstract: A new separation algorithm based on contour segments and ellipse fitting is proposed to separate the ellipse-like touching grain kernels in digital images. The image is filtered and converted into a binary image first. Then the contour of touching grain kernels is extracted and divided into contour segments (CS) with the concave points on it. The next step is to merge the contour segments, which is the main contribution of this work. The distance measurement (DM) and deviation error measurement (DEM) are proposed to test whether the contour segments pertain to the same kernel or not. If they pass the measurement and judgment, they are merged as a new segment. Finally with these newly merged contour segments, the ellipses are fitted as the representative ellipses for touching kernels. To verify the proposed algorithm, six different kinds of Korean grains were tested. Experimental results showed that the proposed method is efficient and accurate for the separation of the touching grain kernels.

Key words: Separation algorithm, Touching grains, Contour segments, Ellipse fitting
doi:10.1631/jzus.C0910797 **Document code:** A **CLC number:** TP391

1 Introduction

With the rising concerns about food quality and safety, computer vision has been increasingly applied for food quality inspection and evaluation because computer vision can provide consistent, cost effective, efficient, and objective measurement (Sun, 2000; Brosnan and Sun, 2004; Aguilera *et al*., 2007). With these advantages, computer vision has been increasingly tested in the inspection and grading of fruit (Paulus and Schrevens, 1999) and vegetables (Shearer and Payne, 1990), and also in the quality evaluation of meats (Lu *et al*., 1997; 2000) and bakery products (Davidson *et al*., 2001). Along with these applications, computer vision has also been widely used in grain quality inspection. Efforts have been made to identify the damaged grain kernels and dockage (Luo *et al*., 1999; Paliwal *et al*., 2003), to classify the grains (Zayas *et al*., 1989; 1996; Paliwal *et al*., 2004a; 2004b; Carter *et al*., 2006), and to inspect and identify rice varieties (Majumdar and Jayas, 1999; Cheng and Ying, 2004a; 2004b; Liu *et al*., 2005; Hobson *et al*., 2007). Most of these studies have been conducted on well-defined images of grain kernels that are placed in a non-touching manner. The clusters of touching grain kernels make the feature extraction and identification of an individual kernel difficult. In the industrial environment, however, such as a vibrating bed, where these systems will finally be implemented, the grain kernels cannot be separated that well; often they touch or even overlap with each other. Therefore, the separation algorithms are needed that split the touching kernels into separated kernels.

Shatadal *et al*. (1995) presented a mathematical morphology-based algorithm to disconnect the conjoint regions in an image of connected kernels. First the progressive erosion was applied, and then

‡ Corresponding author
* Project supported by the Grant of the Korean Ministry of Education, Science and Technology under the Regional Core Research Program

thickening and dilating were used on the eroded images with the constraint that regions belonging to different kernels were not reconnected. But this algorithm was time-consuming and did not perform well on slender grains.

Visen *et al*. (2001) proposed an algorithm based on the potential nodes. The inertial equivalent ellipse was determined first, and then the degree of overlap was calculated to determine whether the component was an isolated kernel or occluding kernels. With the curvature of every boundary point of occluding kernels the potential nodes were identified. Next, the node pairs were constructed with the potential nodes. Finally, the first pair in the sorted list was selected as the terminal points of the segmentation line to separate the connected grains. Gao *et al*. (2007) used a similar method to search concave points and then the split points were matched with judgments of split direction, distance, and synthesis. As the number of touching kernels increased, however, the combinations of potential nodes often failed because of wrong pairings, resulting in wrong segmentation.

Zhang *et al*. (2005a) developed a separation algorithm based on ellipse fitting and clustering to split the connected grain kernels in images. First the object boundary was extracted by the edge detection operator. The edge pixels were tracked and stored in an ordered points list. Every time six of these edge points were randomly selected to fit one ellipse. After 100 fitted ellipses were generated, two selected criteria were applied to eliminate the inappropriate fitted ellipses. Next, the difference and similarity of fitted ellipses were determined by the five main parameters of ellipses, and the ellipses were clustered according to the Euclidean distance between them. Finally, the center patterns of clusters with more than five ellipses were assigned as the representative ellipses. Nevertheless, the algorithm was time-intensive. Moreover, it was tested only with two kernels touching each other. If the number of touching kernels was larger than three, it was difficult to cluster the fitted ellipses and determine the final representative ellipses.

Other algorithms based on Hough transform and morphological transform (Zhang *et al*., 2005b), and distance transform and watershed segmentation (Wang and Paliwal, 2006), had been applied to separate the touching kernels. The former could not solve the above clustering and number problems either, while, for the latter, the internal markers could not be easily found. In addition, both of them were time-consuming.

This paper deals with a new separation algorithm based on contour segments and ellipse fitting to separate the touching grain kernels in digital images. The image is filtered and converted into a binary image first. Then the contour of touching grain kernels is extracted and divided into contour segments with the concave points on the contour. The next step is to merge the contour segments, which is the main contribution of this work. In this part, the distance measurement is proposed to exclude the contour segments with a low possibility that they belong to the same object. The candidate ellipse then is fitted by the direct least square ellipse fitting algorithm, and the deviation error is calculated for evaluating the fitness. Subsequently the contour segments are merged as a new segment if they pass the measurement and judgment. Finally, the ellipses are fitted to be the representative ellipses for touching kernels with these new contour segments. To evaluate our proposed algorithm, six different kinds of Korean grains were used to conduct the experiments and the results show that it is both efficient and accurate in separating the touching grain kernels.

2 The proposed algorithm

The proposed algorithm can be divided into three parts: image pre-processing, contour pre-processing, and contour segments merging. Fig. 1 is the flow chart of the proposed algorithm. Details are described below.

2.1 Image pre-processing

First, the color image is inputted and converted into the grayscale intensity image. Then the median filter is applied on the intensity image to remove the noise because it can protect the edge of the image while removing the noise effectively. Finally, the image is converted into the binary one with the threshold value determined by Otsu's method (Otsu, 1979). The pixels with gray values higher than the threshold are given the value of one as objects; others have the value of zero as background (Fig. 2a).

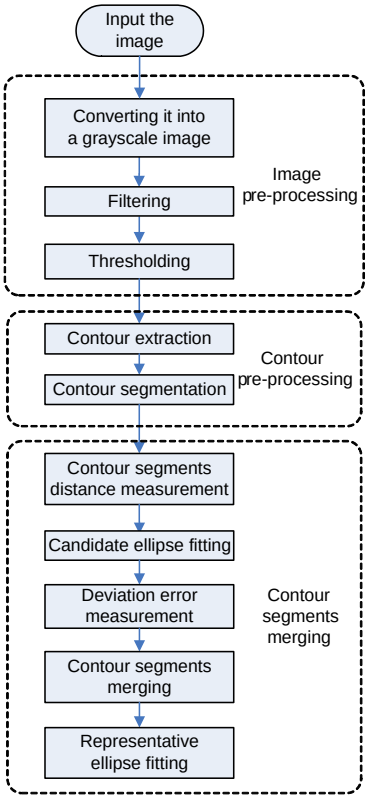

Fig. 1 Flow chart of the proposed algorithm

2.2 Contour pre-processing

With a circular averaging filter the contour of touching kernels in the binary image is smoothed to remove the small-scale fluctuations which may cause false concave points (cp). The contour of touching kernels is extracted by the canny edge detector (Fig. 2b) and the contour points are stored in an ordered list. The following detection method of the concave points is used.

Let $p_t(x_t, y_t)$ be a contour point, and the angle between the lines $\overline{p_t p_{t-k}}$ and $p_t p_{t+k}$ be defined as the concavity of p_t. Here, p_{t-k} and p_{t+k} mean the kth adjacent contour points of p_t; k is set to 2 in this work.

$$\begin{aligned}\text{concavity}(p_t) &= \text{angle}(p_{t-k}, p_t, p_{t+k}) \\ &= \left|\arctan\left(\frac{y_{t-k}-y_t}{x_{t-k}-x_t}\right)-\arctan\left(\frac{y_{t+k}-y_t}{x_{t+k}-x_t}\right)\right|. \quad (1)\end{aligned}$$

The point is determined as the concave point if the following two conditions are satisfied (Fig. 2c): (1) concavity (p_t) is in the range (α_1, α_2); (2) line $p_{t-k}p_{t+k}$ does not traverse the touching kernels.

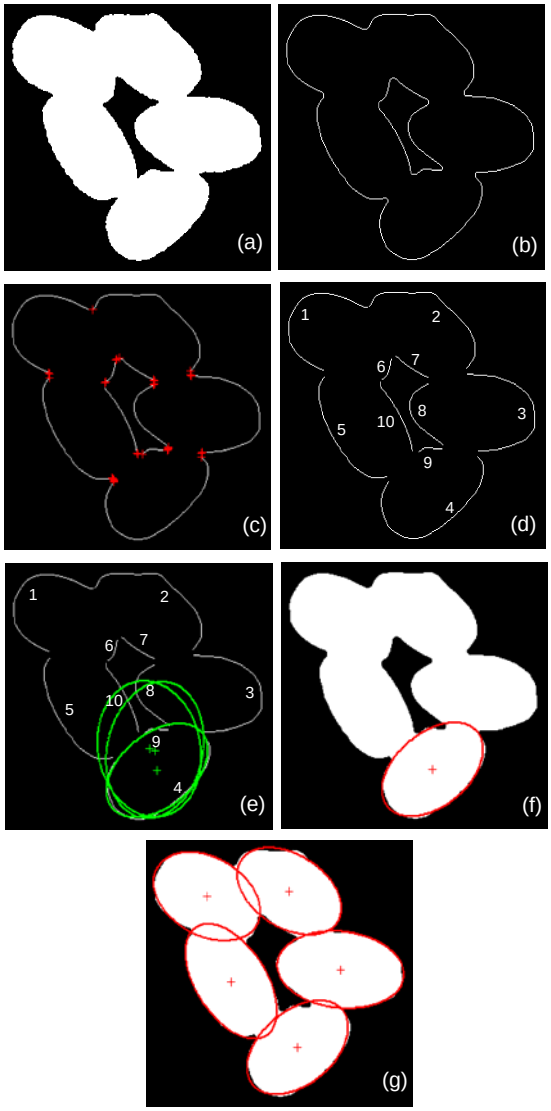

Fig. 2 Processing example of the proposed algorithm
(a) Binary image after image pre-processing; (b) Contour of touching kernels; (c) Concave points on the contour; (d) Contour segments; (e) Candidate ellipses; (f) Representative ellipse of one kernel; (g) Final separation result

The values of α_1 and α_2 are determined as 30° and 150° respectively by the various tests.

With these concave points, the contour (C) of touching kernels can be divided into N contour segments (Fig. 2d).

$$C=\text{CS}_1+\text{CS}_2+...+\text{CS}_N+\text{cp}_1+\text{cp}_2+...+\text{cp}_s, \quad (2)$$

where s is the number of concave points. One contour segment can be represented as $\text{CS}_i=\{p_{i1}, p_{i2},..., p_{iM_i}\}$, where M_i is the number of points $p_{ij}(x_{ij}, y_{ij})$ on CS_i.

2.3 Contour segments merging

From the above processing step, one contour of the same object may be divided into several contour segments. Thus, the aim of this subsection is to merge the contour segments belonging to the same grain. First, several measurements and the ellipse fitting algorithm are introduced, and then the merging steps are explained.

2.3.1 Distance measurement between contour segments

It is obvious that the possibility of two contour segments belonging to the same object is low if the distance between these two segments is large, and vice versa. Hence, assuming this property, the distance measurement is proposed to express the relationship between contour segments to exclude the contour segments with a low possibility of pertaining to the same object.

$$\mathrm{DM}(\mathrm{CS}_i,\mathrm{CS}_j)=\frac{1}{3}[d(p_{i1},p_{j1})+d(p_{im_i},p_{jm_j})+d(p_{iM_i},p_{jM_j})]. \tag{3}$$

Here, $d(p_{i1},p_{j1})$ and $d(p_{iM_i},p_{jM_j})$ are the Euclidian distances between the end points of contours CS_i and CS_j, and $d(p_{im_i},p_{jm_j})$ is the Euclidian distance between the middle points of contours CS_i and CS_j.

2.3.2 Ellipse fitting algorithm

The direct least square ellipse fitting method proposed by Fitzgibbon *et al*. (1999) is applied in this work. A general ellipse can be described by an implicit second-order polynomial:

$$F(x,y)=ax^2+bxy+cy^2+dx+ey+f=0, \tag{4}$$

where

$$b^2-4ac<0. \tag{5}$$

The polynomial $F(x_i, y_i)$ is called the algebraic distance of a data point (x_i, y_i) to the ellipse $F(x, y)=0$. Eq. (4) can be represented in vector form:

$$F(\boldsymbol{k},\boldsymbol{x})=\boldsymbol{x}\cdot\boldsymbol{k}=0, \tag{6}$$

where $\boldsymbol{k}=[a\ b\ c\ d\ e\ f]^{\mathrm{T}}$ and $\boldsymbol{x}=[x^2\ xy\ y^2\ x\ y\ 1]$ are the vectors of the coefficients of the ellipse and the coordinates of the data points, respectively. The coefficients can be found by solving the minimization problem of the sum of squared algebraic distances of the data points to the ellipse

$$E=\sum_{i=1}^{m}F(x_i,y_i)^2, \tag{7}$$

which can be reformulated in vector form as

$$E=\|\boldsymbol{D}\boldsymbol{k}\|^2, \tag{8}$$

where the design matrix $\boldsymbol{D}$ is of size $m\times 6$, and

$$\boldsymbol{D}=\begin{bmatrix} x_1^2 & x_1y_1 & y_1^2 & x_1 & y_1 & 1\\ \vdots & \vdots & \vdots & \vdots & \vdots & \vdots\\ x_i^2 & x_iy_i & y_i^2 & x_i & y_i & 1\\ \vdots & \vdots & \vdots & \vdots & \vdots & \vdots\\ x_m^2 & x_my_m & y_m^2 & x_m & y_m & 1 \end{bmatrix}. \tag{9}$$

It is free to arbitrarily scale the parameters of Eq. (5), so the equality constraint

$$4ab-b^2=1 \tag{10}$$

is imposed. This is a quadratic constraint which may be expressed in the matrix form

$$\boldsymbol{k}^{\mathrm{T}}\boldsymbol{C}\boldsymbol{k}=1 \tag{11}$$

as

$$\boldsymbol{k}^{\mathrm{T}}\begin{bmatrix} 0 & 0 & 2 & 0 & 0 & 0\\ 0 & -1 & 0 & 0 & 0 & 0\\ 2 & 0 & 0 & 0 & 0 & 0\\ 0 & 0 & 0 & 0 & 0 & 0\\ 0 & 0 & 0 & 0 & 0 & 0\\ 0 & 0 & 0 & 0 & 0 & 0 \end{bmatrix}\boldsymbol{k}=1. \tag{12}$$

The vector $\boldsymbol{k}$ could be calculated based on Eq. (11) and the following equation:

$$\boldsymbol{S}\boldsymbol{k}=\lambda\boldsymbol{C}\boldsymbol{k}, \tag{13}$$

where $\boldsymbol{S}$ is the scatter matrix of size 6×6,

$$\boldsymbol{S}=\boldsymbol{D}^{\mathrm{T}}\boldsymbol{D}, \tag{14}$$

and λ is an eigenvalue for $\boldsymbol{S}$.

The sum of squared algebraic distances of the points to the ellipse can be derived as

$$E=\|\boldsymbol{D}\boldsymbol{k}\|^2=\boldsymbol{k}^{\mathrm{T}}\boldsymbol{D}^{\mathrm{T}}\boldsymbol{D}\boldsymbol{k}=\boldsymbol{k}^{\mathrm{T}}\boldsymbol{S}\boldsymbol{k}=\boldsymbol{k}^{\mathrm{T}}\lambda\boldsymbol{C}\boldsymbol{k}=\lambda\boldsymbol{k}^{\mathrm{T}}\boldsymbol{C}\boldsymbol{k}=\lambda. \tag{15}$$

Thus, the eigenvector of $\boldsymbol{S}$ corresponding to the minimal positive eigenvalue λ represents the best-fit ellipse for the given set of points.

2.3.3 Deviation error measurement from the contour segments to the fitted ellipse

In this work, the mean least squared algebraic distance is used as the deviation error measurement, which is proposed to find its fitness evaluation from the contour segments to the fitted ellipse. For the data points of given contour segments $CS^{\#}$, the sum of least squared algebraic distances (E) of the data points to the candidate ellipse CE can be calculated by the above algorithm. Thus, the deviation error measurement can be computed with the following equation:

$$\mathrm{DEM}(CS^{\#}, CE)=E/M^{\#}=\lambda/M^{\#}, \tag{16}$$

where $M^{\#}$ is the total number of points on $CS^{\#}$.

2.3.4 Steps of contour segments merging

With the contour segments of touching kernels, the merging steps are described as follows:

1. Select the longest contour segment CS_l from the contour segments.

2. Construct a set CS^* by including all CS_i if $DM(CS_l, CS_i)<\delta_{DM}$ is satisfied. That is,

$$CS^* = \{CS_i \mid \mathrm{DM}(CS_l, CS_i) < \delta_{DM},\ i = 1, 2, ..., k\}. \tag{17}$$

3. Fit ellipses with CS_l and each CS_i included in CS^* by the direct least square ellipse-fitting algorithm, and compute the DEMs between these two contour segments and their corresponding fitted ellipses.

4. Merge CS_l with all CS_i whose DEMs are smaller than a certain threshold to make a CS_{new}, which can be expressed as

$$CS_{new} = \{CS_l + CS_i \mid \mathrm{DEM}(CS_l, CS_i) < \delta_{DEM},\ i = 1, 2, ..., k\}. \tag{18}$$

5. Fit the ellipse with CS_{new} as the representative ellipse for one of the touching kernels, and delete CS_{new}.

6. Check if all CS_N are detected. If yes, output all representative ellipses and finish the process. If not, go back to Step 1.

To clarify, an example is used to explain the merging steps. Fig. 2d shows the contour segments divided by the concave points. First the longest one among these contour segments, CS_4, is selected. Then the distance measurements are calculated between CS_4 and other CS_i. A set CS^* is constructed with CS_8, CS_9, CS_{10}, for their distance measurements are smaller than a preset threshold δ_{DM}. After that, candidate ellipses are fitted with CS_4 and CS_8, CS_9, CS_{10} respectively, which are shown as the ellipses in Fig. 2e. Subsequently, the deviation error measurements between two contour segments pairs (CS_4 and CS_8, CS_4 and CS_9, CS_4 and CS_{10}) and their corresponding fitted ellipses are computed. Since only CS_9 satisfies condition (18), CS_4 and CS_9 are merged as a new contour segment, and the ellipse is fitted with this new segment and one representative ellipse (the ellipse in Fig. 2f) is the output. Finally, CS_4 and CS_9 are deleted from the contour segments list. These steps are repeated for the longest one in the remaining contour segments, and the steps are looped until all the contour segments are used to fit representative ellipses (Fig. 2g).

Here, δ_{DM} and δ_{DEM} are determined with prior knowledge and various tests. For different kinds of objects, they should be adjusted into different values.

3 Experimental results and discussion

The performance and efficiency of the proposed algorithm have been evaluated. A total of 67 images for six kinds of Korean grains were acquired (9 images for each kind of rice, 15 images for soybean, and 16 images for corn). For each kind, there were 680 kernels of 190 touching objects, among which half of them were used for determining the threshold values and the remaining were used for performance evaluation. The algorithm was implemented with Intel dual core 2.4 GHz CPU, 2 GB RAM. The examples are demonstrated below.

Fig. 3 shows the binary image examples of each kind. Fig. 4 shows the results processed by our proposed algorithm. In these images, there are not only touching chains of grains but also touching clumps with holes (Bailey, 1992), which may not be possible to separate correctly by the preceding techniques. Fig. 4 shows that the cases of touching chains and clumps with holes are all well separated. Moreover, we can see that the proposed algorithm is robust, as it performs well even though the contours of touching kernels are not that smooth.

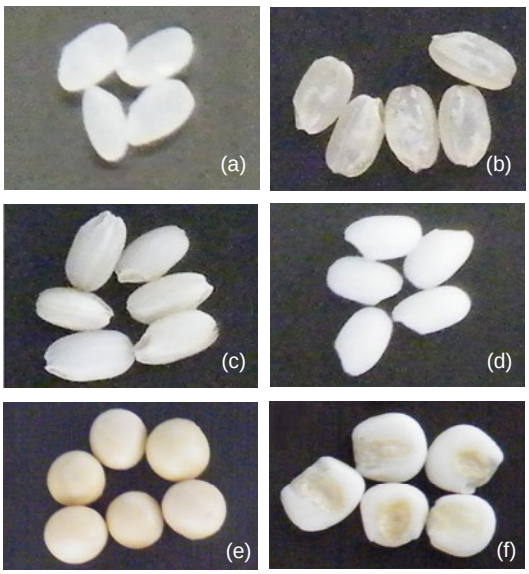

Fig. 3 Image examples of common rice (a), brown rice (b), rough rice (c), glutinous rice (d), soybean (e), and corn (f)

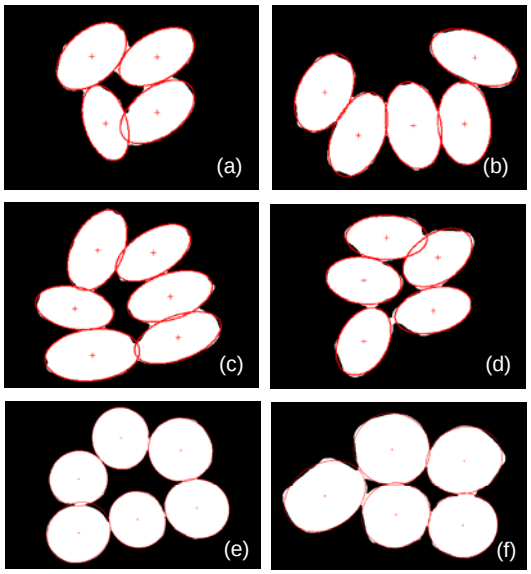

Fig. 4 Experimental results of common rice (a), brown rice (b), rough rice (c), glutinous rice (d), soybean (e), and corn (f)

Table 1 shows the threshold values of distance measurement δ_{DM} and deviation error measurement δ_{DEM} of six kinds of grains.

To evaluate the proposed method, the potential items are tested including:

1. Area overlap measure (AOM), which shows the overlap accuracy of algorithms (Visen *et al.*, 2001). The AOM is calculated with

Table 1 The threshold values

Grain	δ_{DM} (pixel)	δ_{DEM} (pixel)
Common rice	120	200
Brown rice	135	230
Rough rice	130	220
Glutinous rice	130	220
Soybean	320	500
Corn	780	1050

$$\xi = \frac{\mu \cap \upsilon}{\mu \cup \upsilon}, \tag{19}$$

where μ is the number of touching kernels pixels, and υ is the number of the fitted ellipses pixels.

2. Probability of correct detection (PCD), which is the ratio of the number of correctly detected separated grains to the total number of touching kernels in the input image.

The experimental results are shown in Table 2. The mean AOM values for each kind of grain are listed, indicating that the representative ellipses can overlap the touching kernels accurately. The high PCD values show that the algorithm can correctly separate almost all the touching kernels. Therefore, the proposed algorithm is accurate and efficient.

Table 2 The experimental results

Grain	Mean AOM	PCD (%)
Common rice	0.923	94.71
Brown rice	0.937	93.68
Rough rice	0.951	95.29
Glutinous rice	0.929	93.82
Soybean	0.981	100.00
Corn	0.942	96.47

AOM: area overlap measure; PCD: probability of correct detection

Although the experimental results show that the proposed algorithm performs well in separating the touching kernels of six kinds of grains shown above, there are some cases where it cannot achieve correct separation.

One such case is where the grain is not ellipse-like, for example, the buckwheat in Fig. 5. Another case is where some of the contour segments are too short. In the case shown in Fig. 6, the over-segmentation cannot be avoided because the kernels are not strictly elliptical and the inner contour segments of these touching kernels are too short.

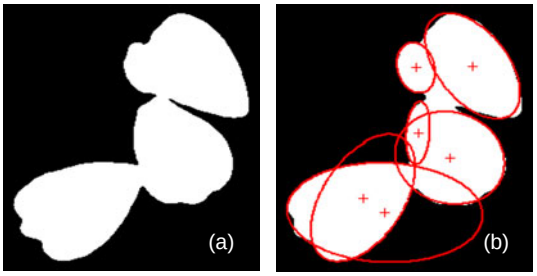

Fig. 5 Examples of buckwheat where the grain is not ellipse-like: (a) original image; (b) segmentation result

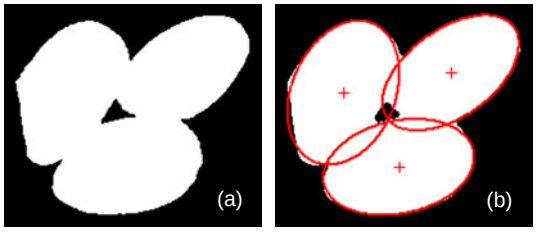

Fig. 6 Examples of short contour segments, where the over-segmentation cannot be avoided: (a) original image; (b) segmentation result

4 Conclusions

A new separation algorithm for the ellipse-like touching grain kernels is developed in this paper. After image and contour pre-processing, the contour of touching grains is divided into several contour segments. Then distance measurement is calculated to exclude the inappropriate contour segments. Next, deviation error measurements are computed to judge the fitness of contour segments and their corresponding candidate ellipses. The satisfied contour segments are merged into a new one, which is used to fit the representative ellipse for the grain. The proposed algorithm is tested with six kinds of Korean grains and the experimental results show that it is efficient and accurate in splitting the ellipse-like touching grains. In addition, this algorithm can not only be used on the color image, but also be conveniently applied on the grayscale or binary image, since it is based on the contour segments of the touching object. Furthermore, the separation result of the proposed algorithm is helpful in positioning the touching grains with the centers of representative ellipses. In the field of identification and classification of grain kernels, it is also helpful if there are some cases where grains are touching with each other because the parameters of representative ellipses can be defined as the features of grains.

References

Aguilera, J.M., Cipriano, A., Eraña, M., Lillo, I., Mery, D., Soto, A., 2007. Computer Vision for Quality Control in Latin American Food Industry: a Case Study. Int. Conf. on Computer Vision: Workshop on Computer Vision Applications for Developing Countries, p.1-11.

Bailey, D.G., 1992. Segmentation of Touching Objects. 7th NZ Image Processing Workshop, p.1-6.

Brosnan, T., Sun, D.W., 2004. Improving quality inspection of food products by computer vision: a review. *J. Food Eng.*, **61**(1):3-16. [doi:10.1016/S0260-8774(03)00183-3]

Carter, R.M., Yan, Y., Tomlins, K., 2006. Digital imaging based classification and authentication of granular food products. *Meas. Sci. Technol.*, **17**(2):235-240. [doi:10.1088/0957-0233/17/2/002]

Cheng, F., Ying, Y.B., 2004a. Machine vision inspection of rice seed based on Hough transform. *J. Zhejiang Univ.-Sci.*, **5**(6):663-667. [doi:10.1631/jzus.2004.0663]

Cheng, F., Ying, Y.B., 2004b. Variety recognition of rice seeds using image analysis and artificial neural network. *SPIE*, **5587**:71. [doi:10.1117/12.570075]

Davidson, V.J., Ryks, J., Chu, T., 2001. Fuzzy models to predict consumer ratings for biscuits based on digital features. *IEEE Trans. Fuzzy Syst.*, **9**(1):62-67. [doi:10.1109/91.917115]

Fitzgibbon, A., Pilu, M., Fisher, R.B., 1999. Direct least square fitting of ellipses. *IEEE Trans. Pattern Anal. Mach. Intell.*, **21**(5):476-480. [doi:10.1109/34.765658]

Gao, H., Wang, Y., Ge, P., 2007. Research on Segmentation Algorithm of Adhesive Plant Grain Image. 8th Int. Conf. on Electronic Measurement and Instruments, **2**:927-930.

Hobson, D.M., Carter, R.M., Yan, Y., 2007. Characterisation and Identification of Rice Grains Through Digital Image Analysis. IEEE Instrumentation and Measurement Technology Conf. Proc., p.1-5. [doi:10.1109/IMTC.2007.379116]

Liu, Z., Cheng, F., Ying, Y., Rao, X., 2005. Identification of rice seed varieties using neural network. *J. Zhejiang Univ.-Sci.*, **6B**(11):1095-1100. [doi:10.1631/jzus.2005.B1095]

Lu, J., Tan, J., Gerrard, D.E., 1997. Pork Quality Evaluation by Image Processing. ASAE Annual Int. Meeting Technical Papers. MI, USA.

Lu, J., Tan, J., Shatadal, P., Gerrard, D.E., 2000. Evaluation of pork color by using computer vision. *Meat Sci.*, **56**(1):57-60. [doi:10.1016/S0309-1740(00)00020-6]

Luo, X., Jayas, D.S., Symons, S.J., 1999. Identification of damaged kernels in wheat using a colour machine vision system. *J. Cereal Sci.*, **30**(1):49-59. [doi:10.1006/jcrs.1998.0240]

Majumdar, S., Jayas, D.S., 1999. Classification of bulk samples of cereal grains using machine vision. *J. Agric. Eng. Res.*, **73**(1):35-47. [doi:10.1006/jaer.1998.0388]

Otsu, N., 1979. A threshold selection method from gray-level histograms. *IEEE Trans. Syst. Man Cybern.*, **9**(1):62-66. [doi:10.1109/TSMC.1979.4310076]

Paliwal, J., Visen, N.S., Jayas, D.S., White, N.D.G., 2003. Cereal grain and dockage identification using machine vision. *Biosyst. Eng.*, **85**(1):51-57. [doi:10.1016/S1537-5110(03)00034-5]

Paliwal, J., Borhan, M.S., Jayas, D.S., 2004a. Classification of cereal grains using a flatbed scanner. *Can. Biosyst. Eng.*, **46**:3.1-3.5.

Paliwal, J., Jayas, D.S., Visen, N.S., White, N.D.G., 2004b. Feasibility of a machine-vision based grain cleaner. *Appl. Eng. Agric.*, **20**(2):245-248.

Paulus, I., Schrevens, E., 1999. Shape characterisation of new apple cultivars by Fourier expansion of digital images. *J. Agric. Eng. Res.*, **72**(2):113-118. [doi:10.1006/jaer.1998.0352]

Shatadal, P., Jayas, D.S., Bulley, N.R., 1995. Digital image analysis for software separation and classification of touching grains. I. Disconnect algorithm. *Trans. ASAE*, **38**(2):635-643.

Shearer, S.A., Payne, F.A., 1990. Color and defect sorting of bell peppers using machine vision. *Trans. ASAE*, **33**(6):2045-2050.

Sun, D.W., 2000. Inspecting pizza topping percentage and distribution by a computer vision method. *J. Food Eng.*, **44**(4):245-249. [doi:10.1016/S0260-8774(00)00024-8]

Visen, N.S., Shashidhar, N.S., Paliwal, J., Jayas, D.S., 2001. Identification and segmentation of occluding groups of grain kernels in a grain sample image. *J. Agric. Eng. Res.*, **79**(2):159-166. [doi:10.1006/jaer.2000.0690]

Wang, W., Paliwal, J., 2006. Separation and identification of touching kernels and dockage components in digital images. *Can. Biosyst. Eng.* **48**:7.1-7.7.

Zayas, I., Pomeranz, Y., Lai, F.S., 1989. Discrimination of wheat and nonwheat components in grain samples by image analysis. *Cereal Chem.*, **66**(3):233-237.

Zayas, I.Y., Martin, C.R., Steele, J.L., Katsevich, A., 1996. Wheat classification using image analysis and crush force parameters. *Trans. ASAE*, **39**(6):2199-2204.

Zhang, G., Jayas, D.S., White, N.D.G., 2005a. Separation of touching grain kernels in an image by ellipse fitting algorithm. *Biosyst. Eng.*, **92**(2):135-142. [doi:10.1016/j.biosystemseng.2005.06.010]

Zhang, G., Deng, J., Jayas, D.S., 2005b. Separation Touching Grain Kernel in Machine Vision Application with Hough Transform and Morphological Transform. CSAE/SCGR Meeting, Paper No. 05-006.